



Copper gettering at half the projected ion range induced by low-energy channeling He implantation into silicon

P. F. P. Fichtner, M. Behar, J. R. Kaschny, A. Peeva, R. Koegler, and W. Skorupa

Citation: [Applied Physics Letters](#) **77**, 972 (2000); doi: 10.1063/1.1289062

View online: <http://dx.doi.org/10.1063/1.1289062>

View Table of Contents: <http://scitation.aip.org/content/aip/journal/apl/77/7?ver=pdfcov>

Published by the [AIP Publishing](#)

Articles you may be interested in

[Gettering of copper in silicon at half of the projected ion range induced by helium implantation](#)

J. Appl. Phys. **91**, 69 (2002); 10.1063/1.1418005

[Evolution of hydrogen and helium co-implanted single-crystal silicon during annealing](#)

J. Appl. Phys. **90**, 3780 (2001); 10.1063/1.1389478

[Investigation of the cut location in hydrogen implantation induced silicon surface layer exfoliation](#)

J. Appl. Phys. **89**, 5980 (2001); 10.1063/1.1353561

[Trans-projected-range gettering of copper in high-energy ion-implanted silicon](#)

J. Appl. Phys. **88**, 6934 (2000); 10.1063/1.1311823

[High-energy ion-implantation-induced gettering of copper in silicon beyond the projected ion range: The trans-projected-range effect](#)

J. Appl. Phys. **88**, 5645 (2000); 10.1063/1.1316054

The image shows the cover of an Applied Physics Reviews journal issue. It features a 3D molecular model of a crystal lattice on the left and a graph on the right. The text 'AIP Applied Physics Reviews' is at the top left, and 'APR-10-2016' is at the bottom left.

NEW Special Topic Sections

NOW ONLINE
Lithium Niobate Properties and Applications:
Reviews of Emerging Trends

AIP Applied Physics Reviews

Copper gettering at half the projected ion range induced by low-energy channeling He implantation into silicon

P. F. P. Fichtner,^{a)} M. Behar,^{b)} and J. R. Kaschny^{a)}

Departamento de Metalurgia, Escola de Engenharia, Universidade Federal do Rio Grande do Sul, POB 15051, 91501-970 Porto Alegre, RS, Brazil

A. Peeva, R. Koegler, and W. Skorupa

Institute of Ion Beam Physics and Materials Research, Research Center Rossendorf, Inc., POB 510119, D-01314 Dresden, Germany

(Received 10 February 2000; accepted for publication 21 June 2000)

He⁺ ions were implanted at 40 keV into Si <100> channel direction at room temperature (RT) and at 350 °C. The Si samples were subsequently doped with Cu in order to study the gettering of Cu atoms at the defective layer. A subsequent annealing at 800 °C was performed in order to anneal the implantation damage and redistribute the Cu into the wafer. The samples were analyzed by Rutherford backscattering channeling and transmission electron microscopy techniques. The Cu distribution was measured by secondary ion mass spectrometry (SIMS). The SIMS experiments show that, while the 350 °C implant induces gettering at the He projected range (R_p) region, the same implant performed at RT has given as a result, gettering at both the R_p and $R_p/2$ depths. Hence, this work demonstrates that the $R_p/2$ effect can be induced by a light ion implanted at low energy into channeling direction. © 2000 American Institute of Physics.

[S0003-6951(00)04133-4]

Metal gettering by ion implantation introduced damage can be used for reducing the concentration of unwanted metal impurities and oxygen in Si. This is called proximity gettering and has been reported by Wong *et al.*¹ The earlier process has been extensively studied in view of its potential application in advanced large scale integration technology.^{2,3} The capture of Cu and Fe contamination in mega-electron-volt implanted Si have been detected by secondary ion mass spectrometry (SIMS) at the depth corresponding to the projected range (R_p) of the implanted ion, where a buried layer of extended defects can be observed by cross section transmission electron microscopy (XTEM).^{4,5} However, in addition to the gettering at R_p , the trapping of Fe and Cu can also be detected at the $R_p/2$ region for Si bombarded with mega-electron-volt ions in the 10^{15} at./cm² fluence range after thermal annealing in the 700–1000 °C temperature interval.^{4–7} This last phenomenon, called the $R_p/2$ gettering effect was observed by Tamura *et al.*⁸ by studying the gettering of O in Czochralski (CZ)–Si after implantation of a variety of ions like C, F, Si, Ge, and As. The $R_p/2$ gettering effect is nowadays attributed to small point defect clusters not visible in TEM images. Their existence is inferred only by means of impurity decoration method.^{9,10} The real nature of the gettering centers at $R_p/2$ is presently discussed in the literature. Most of the authors assume that excess vacancies generated at $R_p/2$ by ion implantation agglomerate in clusters or nanocavities during thermal annealing.^{6–8,11,12} However, more recently, Köegler *et al.*¹³ have suggested that interstitial clusters rather than vacancy ones are responsible for the $R_p/2$ effect. Independent of the earlier controversy, from

the experimental point of view the $R_p/2$ effect is nowadays known to occur for a variety of light-medium ($6 \leq Z_1 \leq 32$) deep ion implants and gettering species.^{9,14}

In the present letter we report on the $R_p/2$ gettering of Cu obtained through a low energy He implant into <100> Si channeling direction. This result seems remarkable since He is a very light ion and it was implanted into a channeling direction. Under such implantation conditions one should expect a significant reduction of the radiation damage at the $R_p/2$ region as compared to the case of heavier ions implanted at mega-electron-volt energies into a random direction, but still the $R_p/2$ effect was observed. On the other hand, we will also show that, upon implantations performed at 350 °C, it is possible to avoid the $R_p/2$ gettering effect caused by the He implants, thus providing new alternatives for the defect engineering applications in He implanted and annealed silicon.

CZ–Si <100> *n*-type wafers with a resistivity of 3–5 Ω were He implanted at 40 keV into Si <100> channeling direction to a fluence $\Phi = 8 \times 10^{15}$ He/cm² at both: room temperature (RT) and 350 °C. Subsequently, Cu was introduced in the rear side of the sample by implanting the Si wafer with 20 keV, 3×10^{13} Cu/cm² at random direction. The samples were then submitted to 800 °C thermal treatment for 600 s in order to anneal the defects and redistribute the Cu into the Si wafer. Rutherford backscattering/channeling (RBS/C) spectrometry was used to characterize the samples after He implantation. The SIMS techniques was employed to determine the Cu depth distribution subsequent to anneal and the extended defect structure (bubbles and dislocations) was characterized by TEM using plan-view and cross section specimens (XTEM).

In Fig. 1 the Cu distribution is shown for the He RT implant together with the corresponding XTEM micrograph.

^{a)}Also with: Instituto de Física, UFRGS.

^{b)}Electronic mail: behar@if.ufrgs.br

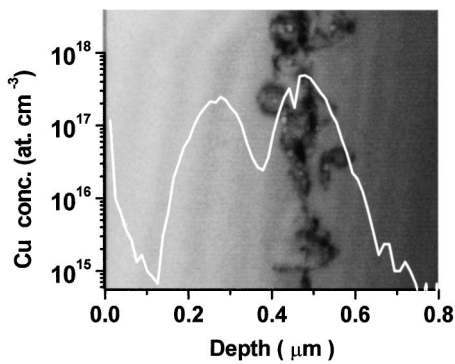


FIG. 1. SIMS analysis of Cu profile superposed with a XTEM micrograph (He implant at RT followed by a thermal treatment at 800 °C for 600 s). Notice the absence of microstructure defects at the region of the shallower peak of Cu and the presence of cavities and dislocation loops at the deeper peak region.

The existence of two Cu peaks can be clearly observed in the SIMS spectrum. The first one located at ≈ 250 nm and the second one at 500 nm. The deeper peak is situated at the region of the He projected range ($R_p = 600$ nm) as deduced from range calculations done via the MARLOWE MONTE-CARLO code.¹⁵ The shallower Cu peak corresponds to the one described in the literature as the $R_p/2$ distribution.^{4–10}

The corresponding XTEM image displays the existence of a well-defined buried layer in the depth range between 400 and 600 nm containing cavities and dislocation loops. This layer is located in the vicinity where the Cu is trapped at the R_p region and no evidence of Cu precipitation was observed. It is worth to note that the TEM investigations do not reveal the existence of any extended defect structure in the vicinity of the shallower Cu peak, which corresponds to the $R_p/2$ region.

Figure 2(a) shows the Cu depth distribution for the He⁺ implant performed at 350 °C together with the corresponding XTEM micrograph. An inspection of the figure reveals the existence of only one Cu peak at the defective region. Due to the low magnification, Fig. 2(a) shows only the strain induced contrast due to the presence of dislocations in the

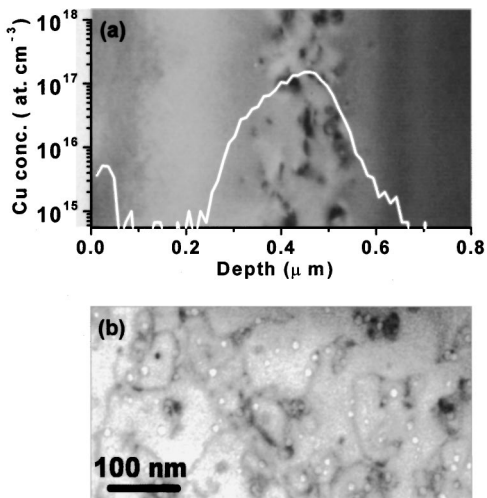


FIG. 2. (a) SIMS analysis of Cu profile superposed with a XTEM micrograph (He implant at 350 °C followed by a thermal treatment at 800 °C for 600 s). Notice that the Cu profile correlates with the region containing strain induced contrast. (b) Plan-view micrograph revealing the presence of cavities and dislocation loop arrangements at the defective layer shown in (a).

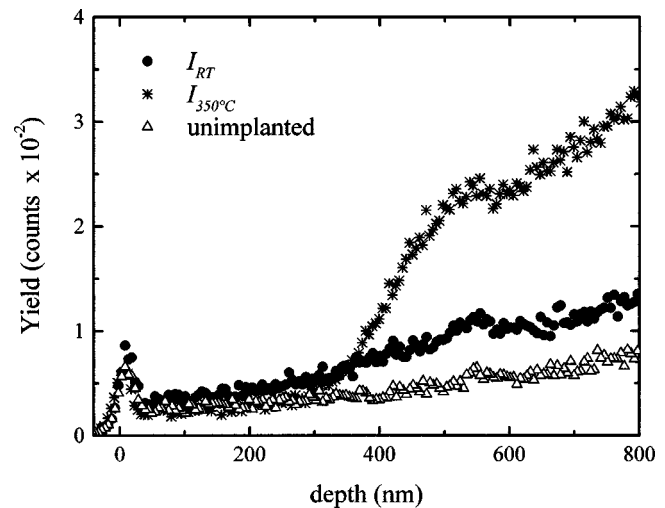


FIG. 3. RBS/C yield vs depth measurements from an unimplanted (Δ) and RT (\bullet) and 350 °C ($*$) implanted samples.

depth layer 300–600 nm. Figure 2(b) shows a more detailed observation of the bubbles and dislocation loops contained in this depth region. It seems interesting to point out that the width of the Cu profile is something larger than the one for RT He⁺ implantation. In addition, the maximum of the Cu profile is slightly shifted towards the surface as compared with the R_p range predictions. This behavior correlates with our observations that, upon high temperature implantation, the He bubbles nucleate not around the R_p position but rather close to the maximum of the radiation induced damage profile.¹⁶

A careful investigation of TEM results reveals quite distinct microstructure features. After annealing, the RT He⁺ implantation give place to a well-defined bimodal He bubble distribution, characterized by a population of large bubbles with a mean radius of 10 nm and a distribution of a smaller ones with a mean radius of 4 nm. Whereas, the 350 °C He⁺ implantation results in a single mode He bubble distribution with a mean radius of 3.6 nm. In addition, the total cavity volume evaluated for each case is also quite different. Expressing the total cavity volume in terms of the quantity of Si atoms displaced in order to open the space for the cavity formation, we have estimated an amount of 2×10^{15} at./cm² for the RT implanted case and 4×10^{14} at./cm² (i.e., a factor 5 smaller) for the high temperature implanted one.

The earlier observations can be correlated with the results of the RBS/C measurements displayed in Fig. 3, which were taken after the He implants but before the thermal annealing treatment. There are shown: (a) the spectra corresponding to an unimplanted sample (triangles), (b) the corresponding to RT He implant (circles), and (c) the one taken for the 350 °C He implanted sample (stars). Comparing (a) and (c) it is observed that up to a depth of ≈ 300 nm there is no difference between the unimplanted and 350 °C spectra. Then, the last one increases its yield significantly at a depth corresponding to the region where the Cu getting starts to be detected. On the other hand, the spectrum corresponding to the RT implantation shows from the near surface up to a depth about 300 nm a yield that is larger than both: the virgin and 350 °C spectra. Near the surface the minimum channeling yield is $\chi_{\min} = 6\%$ (as compared to the virgin sample,

$\chi_{\min}=4\%$) and goes up to $\chi_{\min}=8\%$ at the R_p region.

The results indicate that the channel implant at 350°C —even before the annealing—causes very low radiation damage in the $R_p/2$ region as it is not observable by RBS/C. Probably the radiation induced damage is removed during the implantation process, due to the high implantation temperature. The same does not happen with the damage at the region where bubbles and dislocation loops are formed, as revealed by the RBS/C and TEM observations. Whether He bubbles, extended defects or both are responsible for the gettering process at R_p is an open question that should be further investigated.

Concerning the RT implantation, the RBS/C measurements show that the implantation process leaves a damage region from the near surface going up to the R_p region. The subsequent thermal treatment probably anneals out most of the defects, in particular at the shallower region of the sample, since TEM investigations reveal the existence of extended defects only in the vicinity of the R_p region. However, at variance with the 350°C He⁺ implant, in the present case a Cu peak appears in the $R_p/2$ region indicating the existence of small point defect complexes which should be responsible for Cu gettering in this region. It is possible that these complexes or their precursors are formed by the RT implantation and are not removed by the subsequent thermal process. From this point of view, the present results are quite similar to the previous ones, which have shown the $R_p/2$ effect induced by mega-electron-volt implants.^{4–10}

On the other hand, a comparison between ours and previous mega-electron-volt experiments shows important differences. The present experimental conditions bring as a consequence the introduction of much less primary radiation damage than in the previous cases. MARLOWE calculations for 3.5 MeV Si implanted in Si at random direction indicate that at $\approx R_p/2$ (1.3–1.7 μm) are created approximately 10 Frenkel pairs per incident ion. The same calculations performed for 40 keV He implanted in the $\langle 100 \rangle$ channel direction result in an amount of 0.2 Frenkel pairs per incident ion at $R_p/2$ (0.15–0.30 μm). Then, the primary damage generated at the $R_p/2$ region is about 50 times lower than for the MeV Si⁺ implantation. In spite of that, we still observe a $R_p/2$ gettering effect of the same magnitude as for the MeV Si implanted cases.^{5,10}

It is possible that the $R_p/2$ effect observed in the present work is not caused by the very low radiation damage induced by the He bombardment but rather due to the formation of He bubbles. In fact, it is known that formation of bubbles requires vacancy absorption and/or self-interstitial ejection in order to build the cavities and to relax their internal pressure.¹⁷ Assuming that the dislocation loops around the bubbles and the surface of the Si act as sinks for the ejected interstitials then it can be speculated that some of them may diffuse and agglomerate at the intermediate region that is around $R_p/2$. At this point it seems interesting to remark that, on the basis of the calculations of Heinig and Jaeger,¹¹ the number of interstitial atoms ejected from the bubbles ($2 \times 10^{15} \text{ cm}^{-2}$) was estimated to be at least 10^4 times higher than the number of excess vacancies at the $R_p/2$ region. Hence, at the present, one cannot exclude the possibility that the self-interstitial complexes generated from the bubbles

can play a significant role as gettering sites. Certainly a deeper insight into the kinetics of point defects as well as on the complex nature of the He bubble formation process in Si^{16,17} are necessary in order to answer the question regarding the nature of the defects at the $R_p/2$ region.

In summary, in the present work we have implanted He at low energy in $\langle 100 \rangle$ Si channeling direction at both RT and 350°C . The samples were subsequently contaminated with Cu and submitted to thermal treatment. Cu gettering was observed for He⁺ implantation at 350°C only at the R_p region. For the same implantation performed at RT, Cu gettering appears at both regions, at R_p and around $R_p/2$ regions. The $R_p/2$ gettering effect now established for He implanted at low energy channeling direction shows a similar gettering behavior to the one observed for mega-electron-volt implantation of heavier ions. However, in the present case much less primary radiation damage was generated at the $R_p/2$ region, and still the $R_p/2$ effect of the same order of magnitude as the gettering at R_p was detected. This behavior can be considered as a particular consequence of the He induced cavity formation phenomena. On the other hand, the absence of Cu gettering at $R_p/2$ for the 350°C implantation is ascribed to the damage annealing that occurs during the implantation process. This feature demonstrates a new defect engineering approach on how to avoid the $R_p/2$ effect at once without a need for further thermal treatments.

The authors would like to acknowledge the financial support from the CAPES-DAAD (Brazilian-German) international cooperation program (PROBRAL). One of the authors, P.F.P.F., also acknowledges the support from the Alexander von Humboldt Foundation (Germany).

- ¹H. Wong, N. W. Cheung, P. K. Chu, J. Liu, and J. W. Mayer, *Appl. Phys. Lett.* **52**, 1023 (1988).
- ²J. L. Benton, P. A. Stolk, D. J. Eaglesham, D. C. Jacobson, J. Y. Chang, J. M. Poate, N. T. Há, T. E. Heynes, and S. M. Myers, *J. Appl. Phys.* **80**, 3275 (1996).
- ³A. Agarwal, K. Chistensen, D. Venables, D. M. Maher, and G. A. Rozgonyi, *Appl. Phys. Lett.* **69**, 3899 (1996).
- ⁴S. V. Koveshnikov and G. A. Rozgonyi, *J. Appl. Phys.* **84**, 3078 (1998).
- ⁵R. Kögler, J. R. Kaschny, R. A. Yankov, P. Werner, A. B. Danilin, and W. Skorupa, *Solid State Phenom.* **57–58**, 63 (1997).
- ⁶R. A. Brown, O. Kononchuk, G. A. Rozgonyi, S. Koveshnikov, A. P. Knights, P. J. Simpson, and F. Gonzalez, *J. Appl. Phys.* **84**, 2459 (1998).
- ⁷V. C. Venezia, D. J. Eaglesham, T. E. Haynes, A. Agarwal, D. C. Jacobson, H.-J. Gossmann, and F. H. Baumann, *Appl. Phys. Lett.* **73**, 2980 (1998).
- ⁸M. Tamura, T. Ando, and K. Ohya, *Nucl. Instrum. Methods Phys. Res. B* **59/60**, 572 (1991).
- ⁹O. Kononchuk, R. A. Brown, S. Koveshnikov, K. Beaman, F. Gonzales, and G. A. Rozgonyi, *Solid State Phenom.* **57–58**, 69 (1997).
- ¹⁰R. Kögler, D. Panknin, W. Skorupa, P. Werner, and A. B. Danilin, *Conference Proceedings of XI International Conference on Ion Implantation and Technology-96 IEEE Publ. 96TH8182 Piscatawg, NY* (1996).
- ¹¹K.-H. Heinig and H.-U. Jaeger (private communication).
- ¹²O. W. Holland, L. Xie, B. Nielsen, and D. S. Zhou, *J. Electron. Mater.* **25**, 99 (1996).
- ¹³R. Kögler, A. Peeva, W. Anwand, G. Brauer, P. Werner, U. Goesele, and W. Skorupa, *Appl. Phys. Lett.* **75**, 1279 (1999).
- ¹⁴R. Kögler, R. A. Yankov, J. R. Kaschny, M. Posselt, A. B. Danilin, and W. Skorupa, *Nucl. Instrum. Methods Phys. Res. B* **142**, 493 (1998).
- ¹⁵M. T. Robinson, *Nucl. Instrum. Methods Phys. Res. B* **48**, 408 (1990).
- ¹⁶P. F. F. Fichtner, A. Peeva, M. Behar, G. de M. Azevedo, R. L. Maltez, R. Kögler, and W. Skorupa, *Nucl. Instrum. Methods Phys. Res. B* **161–163**, 1038 (2000).
- ¹⁷P. F. F. Fichtner, J. R. Kaschny, R. A. Yankov, A. Mucklich, U. Kreißig, and W. Skorupa, *Appl. Phys. Lett.* **70**, 732 (1997).